

**Stability assessment of rock slopes combining Slope Mass Rating and Qslope
classification systems: A case study in Cerro San Eduardo
(Guayaquil, Ecuador)**

Alexandra Monserrate Macías Macías. Escuela Superior Politécnica del Litoral
(ESPOL) Guayaquil. Ecuador. almomaci@espol.edu.ec,

Dalida Kaymara Vera Quiroz. Escuela Superior Politécnica del Litoral (ESPOL)
Guayaquil. Ecuador dkvera@espol.edu.ec

César Patricio Borja Bernal. Universidad de Guayaquil. Ecuador.
cesar.borjab@ug.edu.ec

Luis Jordá-Bordehore. Universidad Politécnica de Madrid. Spain. l.jorda@upm.es

ABSTRACT

In the present study, the stability of the slope located in the Modesto Apolo Ramírez Avenue, is analyzed. The avenue is located prior to the access to the Cerro San Eduardo tunnel, which has had habitual problems of falling blocks to the roadway. For the study, empirical methodology was applied, including the data mapping based on geomechanical classifications such as Rock Mass Rating (RMR), Slope Mass Rating (SMR) and Q-Slope index, which assign a defined score, obtaining the quality of the rocky mass, and with this, the degree of stability of the slope. In addition, through the application of RocFall software, the empirical methodology has been compared with the analysis of rockfall trajectory, making a retrospective study of behavior and simulating the constant falling of blocks on the roadway.

As a consequence of the exploration, it was evident that the geomechanical classifications -in this particular case- are not completely effective to determine the degree of stability of the massif. This is due to the fact that, even though the slopes are globally stable, these classifications do not seem to adequately determine a level of risk against rockfalls, as can be seen from visu. Therefore, it can be seen that the slope does not have a risk of collapse, but instead presents a high danger of landslides that could cause considerable economic and human lives losses. The study recommends geometric solutions for impact mitigation to prevent future damage.

Keywords- RMR, SMR, Q-Slope, stability, massif, impact.

1. INTRODUCTION

The study of rock slope instability can be explained with kinematic analysis, boundary equilibrium, numerical modeling and empirical methods (Basahel and Mitri, 2017). The main problem presented by the researchers is the selection of an appropriate method for each type of instability, with the aim of simplifying a complex reality and integrating different forms of breakage. In the last 30 years, different geomechanical classifications and empirical analyses of slope stability (planar, wedge, overturning, etc.) have emerged as a preliminary analysis of the stability of the massifs.

In 1973, Bieniawski introduced the Rock Mass Rating (RMR) geomechanical classification system with its successive versions (Bieniawski, 1976, 1979, 1984, 1989), improving the characterization method. Yet, this method is used in tunnels (Bieniawski, 1993), and is not particularly applied in slopes due to the scores for the orientations of the discontinuities do not have a guideline for the definition of each class. It involves greater ranges of errors in this value and therefore the classification work becomes complicated and arbitrary (Romana et al., 2003).

From the RMR, Romana (1985) developed the Slope Mass Rating SMR, which introduces factors that correct the basic RMR for slopes; improving the method in 1995. On the other hand, Barton in 1974 developed the Q-index for tunnels (Barton et al., 1974), where the mass is characterized according to some parameters. Nevertheless, in 2017 Bar and Barton developed a new method modifying some parameters of the Q-index, in which they addressed the application of the same one to slopes in rock called Q-slope (Bar and Barton, 2017).

The main advantage of these empirical methodologies lies in their simple applications both in the design stage and in the execution of work. However, it is essential to know the limitations of geomechanical classifications (Palmstrom and Broch, 2006; Fernández-Gutiérrez et al., 2017) since their application in certain massif conditions are not able to replace more accurate and refined designs and calculations. (Jordá-Bordehore, 2017).

Given the population growth of the city of Guayaquil, there is a need for roads that communicate certain populated areas, which is the case of the Modesto Apolo Ramírez Avenue. The avenue has a slope located on the right side, prior the entrance of the tunnel San Eduardo in the north-south direction, where the hill of the same name is located. This hill has an exposed slope of considerable height, with a limestone - diaclastic lithology and presence of fragments of clay and silty rocks, which leads to constant slides of exposed blocks. This generates a situation of risk for the users of the road and urges the present stability analysis.

In the present research, geomechanical classifications RMR, SMR, and Q-slope were used to determine the stability of the rock masses. In addition, the application of empirical methods is contrasted against slopes with a considerable degree of fracturing and, is included as well, given the particular geological condition, an analysis by falling blocks. This comparison strengthens the current approaches and recommendations that suggest the application of empirical methods as a starting point for outlining a problem of instability. So, they allowed directing the study in such a way that it reaches the ideal solution by means of analytical or numerical methods. (Jordá-Bordehore et al., 2017)

2. GEOLOGICAL SETTING

The study area is situated southwest of the city of Guayaquil, at Km 14.5 of the coast road, on the sides of Modesto Apolo Ramírez Avenue, which was built as a bypass to the San Eduardo tunnel. The zone of interest corresponds to the Cayo and the Guayaquil Member formations. Both formations of Senonian and Maestrichtian age (Bristow, 1976) of the Cretaceous superior to the Eocene, with wide sequences and thin stratifications with dipping predominantly towards the south. (Instituto Geográfico Militar, 2020). The area of study is shown in Fig. 1.



Fig 1. Orthophoto of the study area.

In these formations, fine brown volcanic sandstones, black silica shales and sedimentary tuffs predominate in successive layers of 0.3 m average thickness with an extension of approximately 80 km in the west to the province of Santa Elena. (Bristow and Hoffstetter, 1977; Navarrete, 2018).

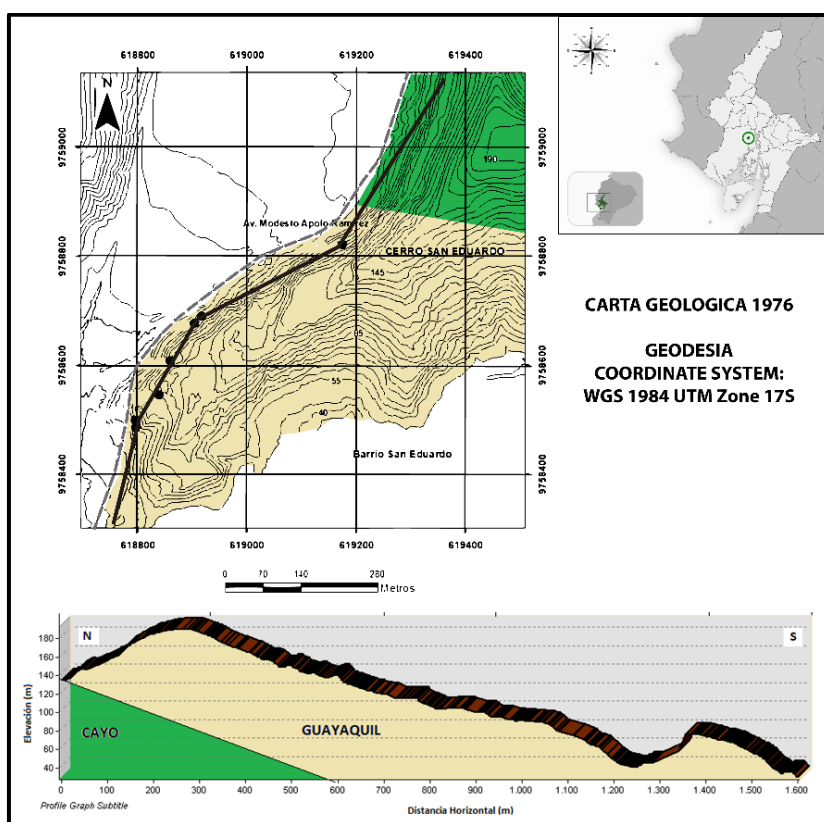


Fig 2. Location map of the study area with the characteristic geological formation.
Modified on: Instituto Geográfico Militar, 2020.

2.1. Slide zones

In the plan view of figure 2, the altimetry detail of San Eduardo Hill is also shown. In the area near the road, the concentration of contour lines can be observed, which corresponds to elevations of up to 130 meters with slopes greater than 40°, susceptible to landslides, which is why it is considered a moderate landslide risk area. (Instituto Geográfico Militar, 2020).

3. METHODOLOGY

3.1 Geomechanical characterization

In order to carry out the analysis of the stability of the slope of Cerro San Eduardo, the application of empirical methods or geomechanical classification (RMR, SMR and Q-Slope) has been considered, thus evaluating the possibility that the slope may have to slide according to the different breakage scenarios that are known (flat breakage, wedge breakage, overturning of strata or circular breakage) (Pantelidis, 2009) and determining the adequate inclination that the slope must have in order to maintain its optimum stability. Geomechanical stations have been carried out in which the parameters of both classifications are taken, as well as other useful parameters such as the resistance to cutting of the joints and the rock matrix.

3.2 Rock Mass Rating, RMR

This classification system was developed by Bieniawski in 1973, who supported the method by reviewing more than 300 real cases of subway works. To determine the RMR index of rock quality, six parameters of the massif must be obtained, which obey a ranking that ranges from 0 to 100 points where the higher the score, the better the rock quality; and according to the classification obtained, certain geotechnical characteristics of the massif can be determined (angle and cohesion) and its behavior in front of excavations (Bieniawski, 1989). The factors that are reviewed in the RMR index are the following:

1. The simple compressive strength of the material
2. The Rock Quality Designation, RQD. (Deere & Deere, 1988)
3. The spacing of the discontinuities
4. The state of the discontinuities
5. The presence of water
6. The orientation of the discontinuities, according to each case (foundations, tunnels or slopes).

Bieniawski, also proposes approximations of the classes of rock according to the value of the RMR.

- CLASS I: $RMR > 80$, Very good rock
- CLASS II: $80 > RMR > 60$, Good rock
- CLASS III: $60 > RMR > 40$, Medium rock
- CLASS IV: $40 > RMR > 20$, Bad Rock
- CLASS V: $RMR < 20$, Very bad rock.

3.3 Slope Mass Rating, SMR

The Slope Mass Rating (SMR) classification was included as a slope analysis method by Romana (1985) starting from Bieniawski's RMR geomechanical classification widely used in tunnels but which presents the limitation for its application in slopes due to the importance of joints (Romana, 1995). The SMR introduces four adjustment factors based on the geometry of the discontinuities with respect to the slope and the excavation method that it presents, allowing

to correct the RMR, determining a description of the quality of the mass, its stability, breakage and recommended treatment (Romana et al., 2001). For these effects, the following equation is used:

$$SMR = (RMR_{basic}) + (F1 \times F2 \times F3) + F4 \quad (1)$$

Where:

F1: Depends on the parallelism between the direction of the joints or discontinuities and the plane of the slope. It varies between 1.0 and 0.15.

F2: Depends on the dip of the joint. In the case of flat breaks, it varies between 1.0 and 0.15. It has a value of 1.0 for breakages by overturning.

F3: Reflects the relationship between the joint dip and the slope.

F4: Values the method of excavation of the slope, varying from a natural slope to -8 in a slope with deficient blasting.

Table 1.

Seal adjustment factors by SMR method. Modified from Romana (1985) by Anbalgan et al. (1992)

Type of break		Very favorable	favorable	Normal	Unfavorable	Very unfavorable
P	$ \alpha_j - \alpha_s $	> 30	30 - 20	20 - 10	10 - 5	< 5
T	$ \beta_j - \alpha_j - \alpha_s $					
W	$ \alpha_i - \alpha_s $					
P/T/W	F1	0,15	0,40	0,70	0,85	1,00
P/W	$ \beta_i \text{ o } \beta_j $	< 20	20 - 30	30 - 35	35 - 45	> 45
P/W		0,15	0,40	0,70	0,85	1,00
T	F2			1,00		
P	$\beta_j - \beta_s$	> 10	10 - 0	0	0 - (-10)	< (-10)
W	$\beta_i - \beta_s$					
T	$\beta_j + \beta_s$	< 110	110 - 120	> 120	-	-
P/W/T	F3	0	-6	-25	-50	-60

Adjustment factor for excavation method F4				
Method	Natural slope	Precut	Blasting soft	Blasting or digging mechanics
F4	+15	+10	+8	0

Table 2.

Stability classes and classification of rocky slopes according to SMR (Romana, 1985).

Class No.	V	IV	III	II	I
SMR	0 - 20	21 - 40	41 - 60	61 - 80	81 - 100
Description	Very bad	Bad	Normal	Good	Very good
Stability	Totally unstable	Unstable	Partially stable	Stable	Totally stable
Probability of breakage	0.9	0.6	0.4	0.2	0
Breaks	Large breakages plans continuous or mass	Joints or large wedges	Some joints or many wedges	Some blocks	None
Treatment	Re-excavation	Correction	Systematic	Occasional	None

3.4 Q-slope Index

The Q-slope system is a new classification of rock masses applied specifically for rock cuts or slopes and is based on the Q index. The Q-slope uses the same six parameters RQD, Jn, Jr, Ja, Jw and SRF as the Q index (Barton and Bar 2015). But also considers the relationships between roughness and filling of wedge-forming joints (Jr/Ja) and their discontinuity orientation factor (0). Moreover, the water parameter (Jw) is replaced by the long-term exposure factor to various climatic and environmental conditions of the slope (Jwice). Some Stress Reduction Factor (SRF) categories relevant to the surface of the slope are also reviewed and applied on a case-by-case basis. (Jordá-Bordehore, 2017). The equation used for the Q-slope is: (Bar & Barton, 2017)

$$Q_{slope} = \frac{RQD}{J_n} \left(\frac{J_r}{J_a} \right)_0 \frac{J_{wice}}{SRF_{slope}} \quad (2)$$

Where:

Jn= Diaclasate index.

Jr= Roughness index

Ja= Alteration index.

Jw= Reduction coefficient due to the presence of water.

0= Discontinuity orientation factor.

SRF= Stress reduction factor.

After the calculation of Q-slope, the evaluation of the slope stability is made from the graph β vs Q-slope proposed by Bar & Barton in 2017. The calculation was based on more than 200 retrospective data analysis in igneous, sedimentary and metamorphic soils around the world (Bar & Barton, 2016), for which, it is required to verify in advance the actual dipping angle " β ", to keep the rock mass stable. (figure 5) (Jordá-Bordehore, 2017). Where:

$$\beta = 20 \log_{10}(Q_{slope}) + 65^\circ \quad (3)$$

3.5 Falling blocks

The instabilities due to falling blocks occur when one of them is suddenly released from one of the apparently solid faces as a product of relatively small deformations in the rock matrix, and they occur when the forces acting on the discontinuities isolate the block from its neighbors and it is released from the surface where it was attached, sometimes they can be of great size. (Guzzetti et al., 2003; Hoek, 2000).

For the analysis it is necessary to consider several parameters, among them, the most important and that controls the trajectory and scope of the fall, is the geometry of the slope. The average mass of the blocks and the state of the faces of the slope, also have a considerable impact, since if these are of unweathered hard rock and without abundant vegetation there is no opposition to the movement. On the other hand, the covered surfaces absorb a portion of the block's potential energy, which would dissipate the amount of bounce and consequently reduce the range. (Hoek, 2000; Hantz et al., 2003).

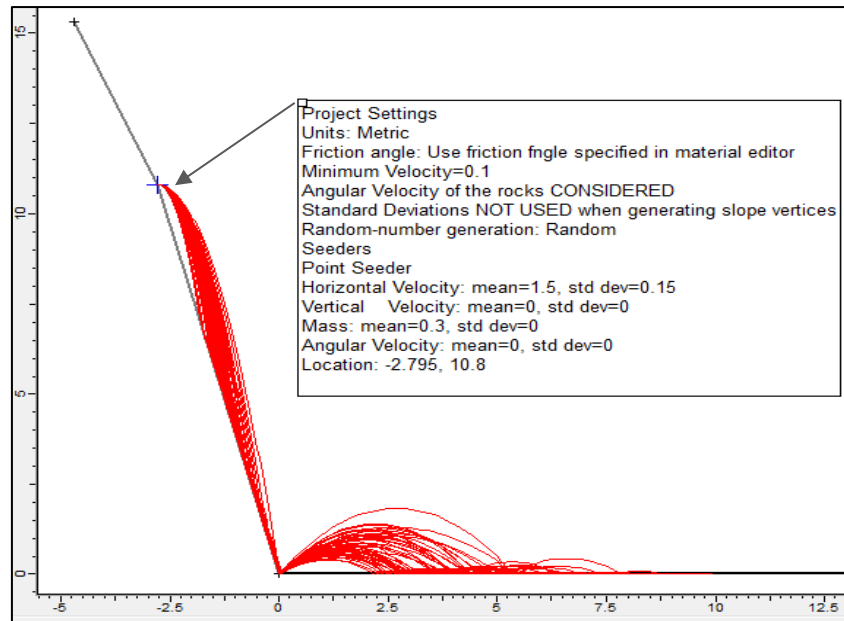


Fig 3. Drop path of 50 blocks of 0.3 Kg. Modified on: Rocfall program.

4. FIELD WORK AND RESULTS

4.1 Geomechanical stations and previous kinematic analysis

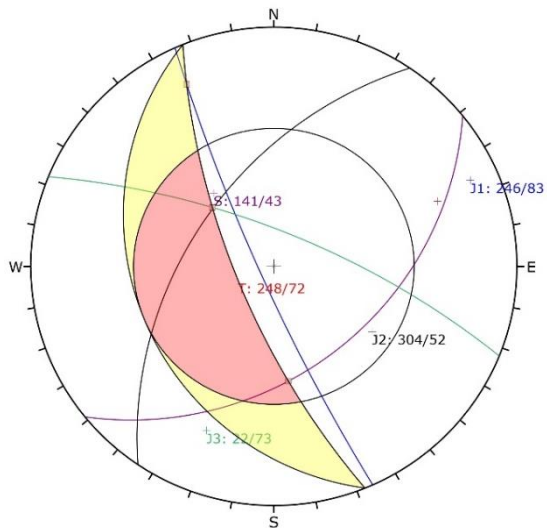
There were 4 geomechanical stations, divided by the significant change of structural domains in each zone. For each one of them, the information of a profile, dipping and diving direction of the main families of discontinuities was collected. In this way, with the input of the data collected in the Dips 6.0 software, it was possible to obtain stereographic projections with the concentrations of poles according to each station and to group them in families. By cinematically analyzing each part of the slope, the possible types of faults that could occur in each sector were made evident.

For the kinematic breakage analysis, geotechnical parameters of hard shales were considered. Since there is no data on friction angle or specific weight of the rock, these values are assumed according to references (Hoek and Bray, 1981), which establish a range of 25-35° for the friction angle in the case of soft sedimentary rocks. It was assumed an intermediate value of 30°, which stands for sandstones, shales, and siltstones. This value will be used as a friction circle in the kinematic model. In Fig. 4, are presented the stereographic projection where details the specific breakage for each station.

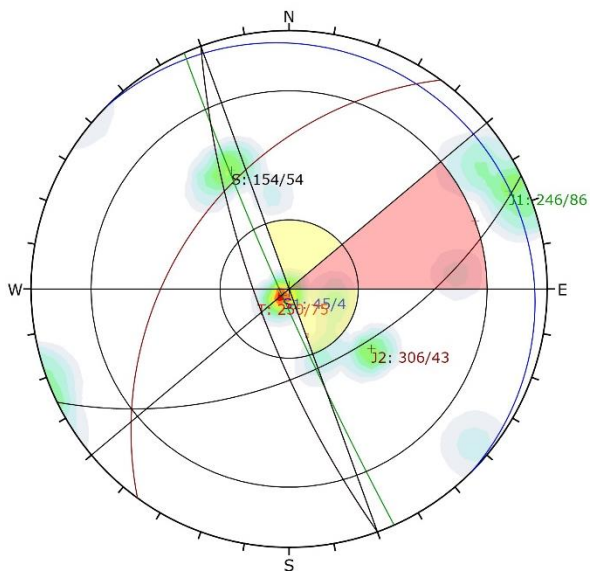
The kinematic analysis requires the type of breakage being analyzed to be established a priori (SMR), and knowing whether the structure is stable or not (Q-Slope). Considering the information obtained in this analysis and knowing that the most predominant discontinuity of the slope in all geomechanical stations corresponds to the stratification plane, it is necessary to verify the degree of instability represented by each type of failure in the stations examined.



(a) GS-1



(b) GS-2



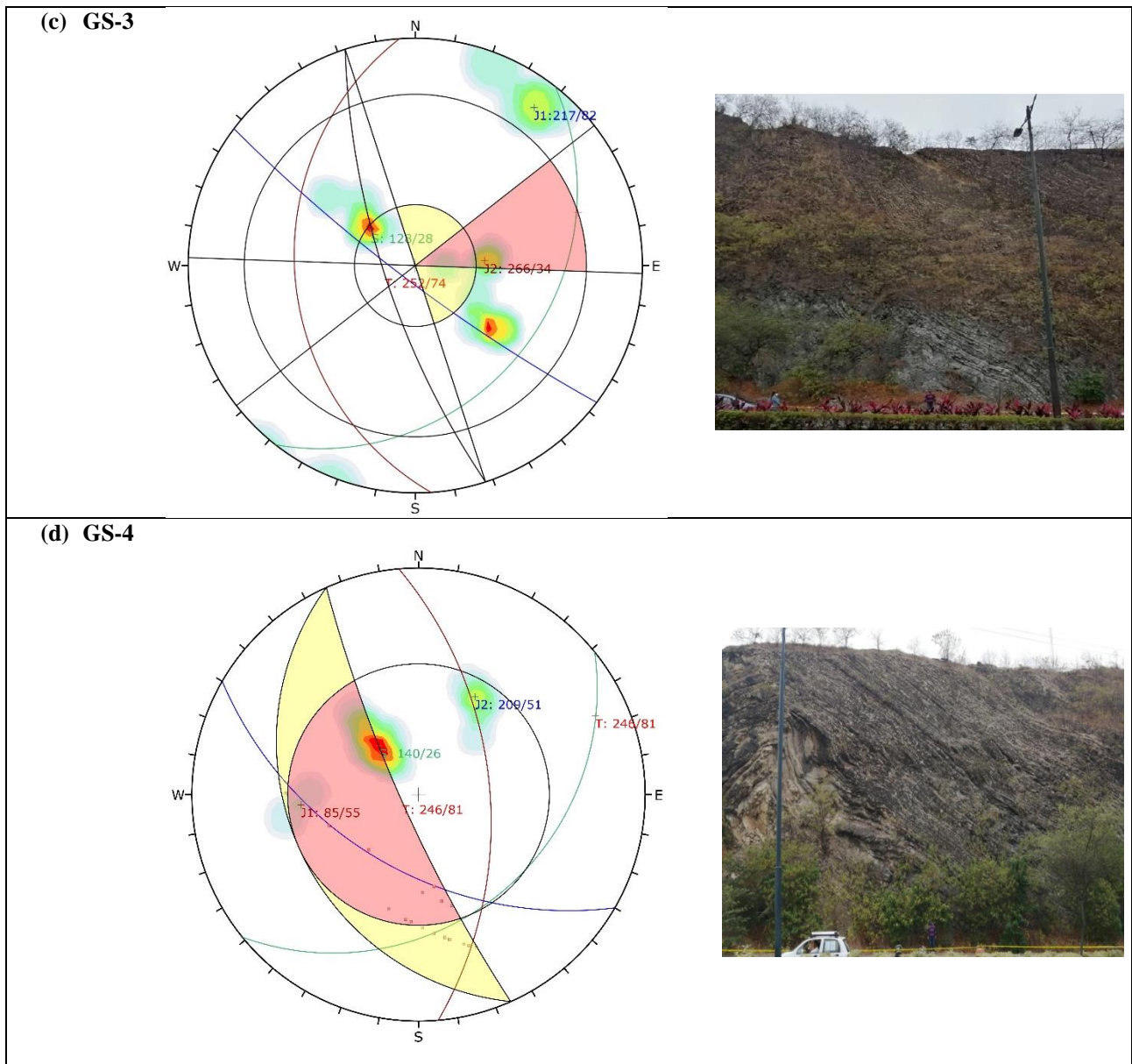


Fig. 4. Diagram of pole density and breakage typologies with representative photographs of the stations. (a) GS-1 instability due to wedge type failure; (b) GS-2 instability due to toppling type failure; (c) GS-3 instability due to toppling type failure; (d) GS-1 instability due to wedge type failure. Modified on: Dips 6.0 program.

As can be seen, in the GS-1 and GS-4 stations the most visually evident type of instability is the wedge, this statement is verified with the kinematic analysis performed (Fig. 4a and 4d). Stations GS-2 and GS-3 present a different type of breakage from the wedge: it is a failure by overturning in both zones, also observing that in certain sectors of the latter stations there is a greater presence of falling blocks apparently produced by the overturning of these (Fig. 4b and 4c).

4.2 Results of Methods used

Once the families of discontinuities and the types of instabilities or ruptures most likely to occur in each station have been obtained, the slope is evaluated using the empirical methods described above (Table 3, Table 4).

4.2.1. RMR:

To determine the SMR, it was necessary to previously calculate the basic RMR of each station. It was possible to find out that in general, all the slopes presented a class of rock Type III, which corresponds to an average quality. This matched with the field experience, as sectors with intact rock were found and resistances that ascended up to 68 MPa were evidenced, considered an acceptable value within the geotechnical characteristics of a sedimentary formation.

Table3

RMR Classification Results.

Geomechanical Stations	Height of the slope	Dip Dir /Dip of the slope face	RMR							RMR basic	Quality of the rock
			RMR-1	RMR-2	RMR-3	RMR-4	RMR-5	Diaclose State	Water		
			Simple compr. strength	RQD	Spaced						
GS-1	12	248/72	4	13	8	14	15	54	Type III (Medium)		
GS-2	23	250/75	7	8	8	11	15	49	Type III (Medium)		
GS-3	19	252/74	4	8	8	15	15	50	Type III (Medium)		
GS-4	15	246/81	4	8	8	15	10	45	Type III (Medium)		

4.2.2. SMR and Q-Slope:

Whenever the basic RMR of each station is obtained, the SMR is calculated. Once the SMR value is obtained, and considering that the mechanism of breakage has been determined a priori (previous kinematic analysis), the classification results suggest that all the studied areas obey to a "Class III" category, as detailed in Table 4. The category suggests that the massif responds to a normal quality with partial stability; its probability of breakage would be triggered by some joints or many wedges and the type of treatment to be received to avoid damage would be one of a systematic nature. It is presumed that this classification does not precisely define the situation analyzed as the methodology does not consider the falling blocks. The Q-slope system (Table 4) was also applied, which indicates:

- a) The slope at stations 1, 2 and 3, is within the stable limits, as shown in Fig. 5. Therefore no correction measures are required on the frontal side of the slope, according to each zone analyzed.

b) Sector 4 presents partial stability and it is situated at the limit towards the zone of uncertain stability (Fig. 5). However, considering that the location of the uncertainty is oriented towards the stable zone, it is determined that the slope does not require greater correction in its dip angle either.

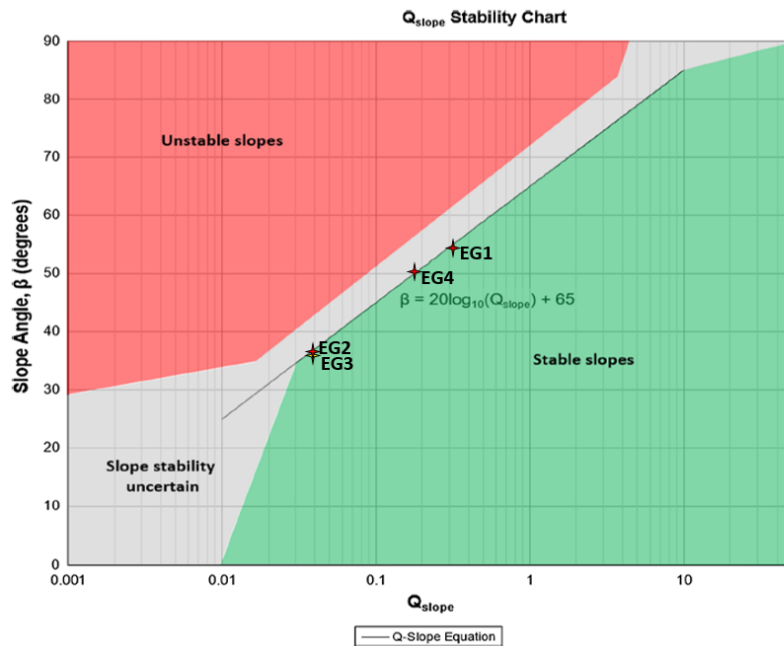


Fig. 5. Presentation of the stability of the slopes of each geomechanical station. Modified on: Bar and Barton, 2017.

Table 4

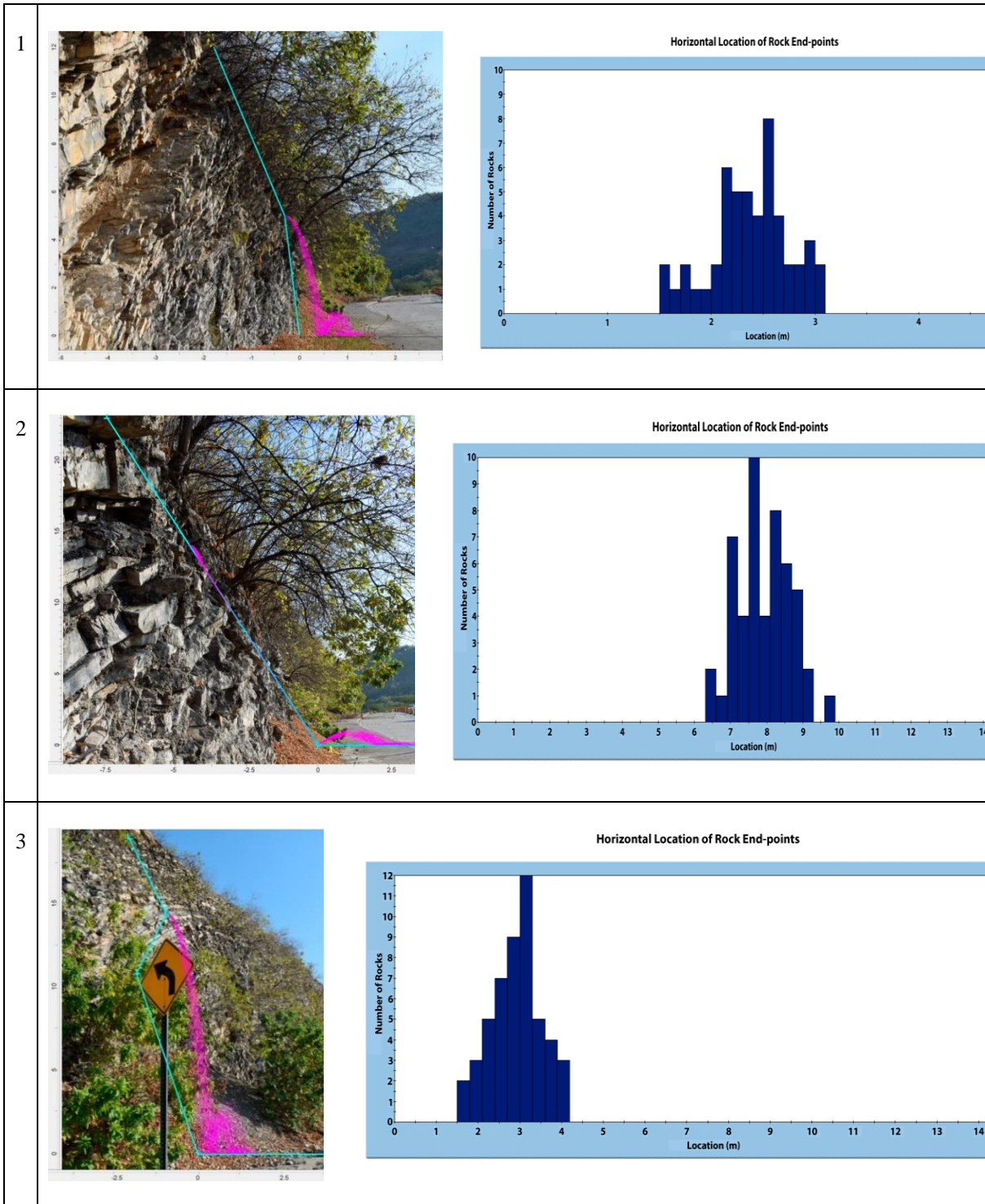
Results of SMR and Q-slope systems for the Cerro San Eduardo - Guayaquil slope stations.

Geomechanical Stations	SMR						Q-slope							
	F1	F2	F3	F4	SMR	Rock Stability	RQD	Jn	$(\frac{Jr}{Ja})_0$	Jwice	SRFslope	Qslope	β	Slope stability
GS-1	0.15	1.00	-60.00	10.00	55.00	Class III - Partially Stable	73	12	0.38	0.65	5	0.3	54.55	Stable
GS-2	0.15	1.00	-25	10.00	55.25	Class III - Partially Stable	41	12	0.094	0.65	5	0.042	37.39	Stable
GS-3	0.15	1	0	10.00	60	Class III - Partially Stable	40	12	0.094	0.65	5	0.041	37.18	Stable
GS-4	0.15	1	-60	10.00	46	Class III - Partially Stable	33	9	0.38	0.65	5	0.18	50.15	Partially Stable

4.3. Rock Masses Detachment

When verifying that the different methods suggest that the slope is globally stable, emerge the concern to re-examine them in a meticulous form, since it is observed that there is high presence of falling rocks due to the important fragmentation to which it is put under. Knowing this particularity, a rockfall analysis is performed with Rocfall software to determine the behavior and scope of the blocks detached from the slope and how much they could affect the surrounding area. Later, the general stability was also evaluated as the fall of successive blocks

and fragments can cause a collapse of the slope due to the “domino effect”. This type of analysis does not seem to be feasible with the empirical methodologies of SMR or Q-slope.



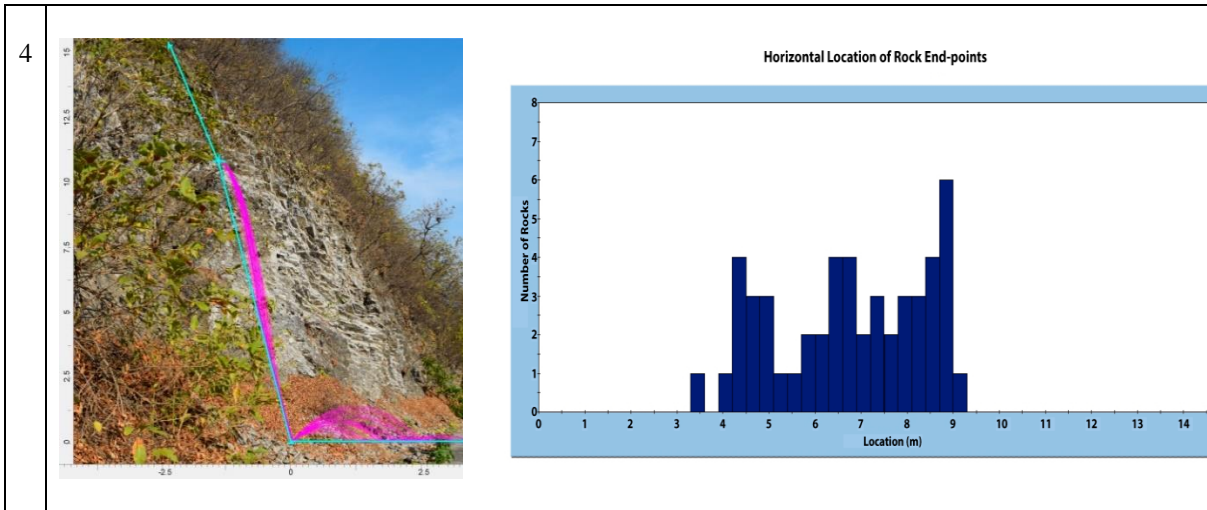


Fig. 6. Schematic and block range distribution of the Geomechanical Stations.
Modified on: Rocfall.

For this purpose, during the field activities to collect information, blocks of varied sizes were observed. However, there is a large portion of small masses of about 0.3 kg. These blocks are separated from the massif apparently for inactivity. Still, the internal forces print a horizontal force which favors the falling blocks, estimated at 0.15 m/s (Rocscience, 2002).

Given the geometry of each profile, estimated from the topography and the use of a compass, there are different behaviors during the fall. A more critical situation is observed in profile 2, from Fig. 6. Likewise, are presented the trajectories of falling rocks and its reach density diagrams for each station.

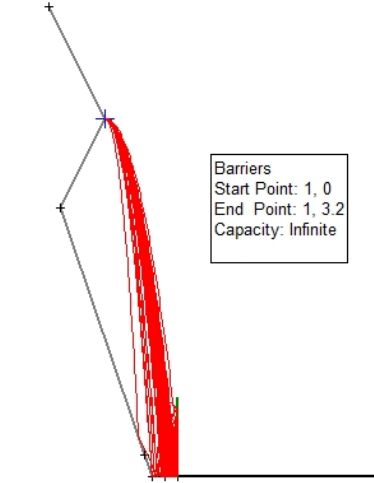
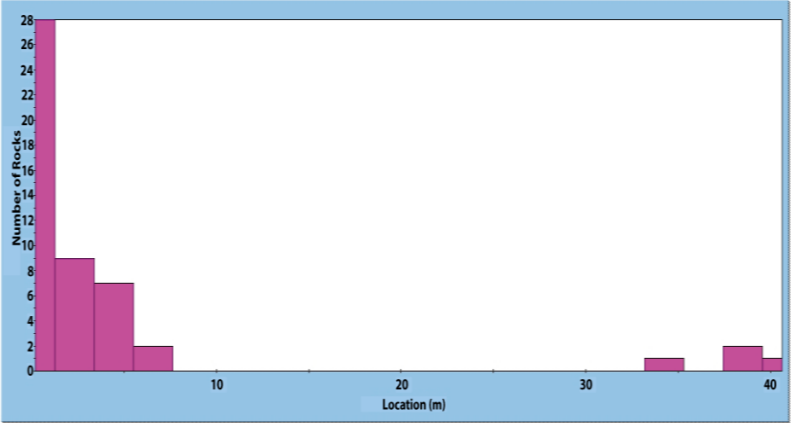
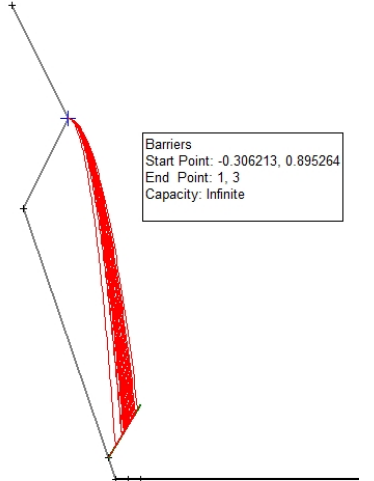
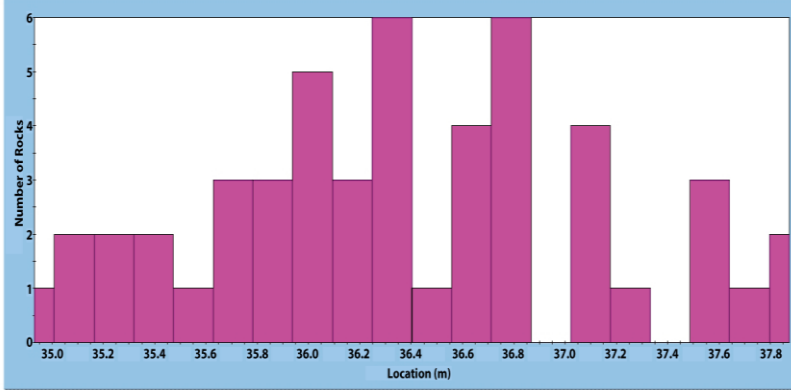
In Fig. 6, a particular behavior is observed in profile 2, where the rocks slide down the slope, so the kinetic energy gives a greater length of intrusion to the roadway, but reaches a lower height after the first bounce. In this model, the maximum height of 1 meter and horizontal reach of approximately 3 meters can be observed, taken from the base of the slope.

The profile registered in Geomechanical Station 3 must be considered as a critical case. In this profile, a section is shown with a counter-slope in the cut, and as a consequence, the blocks acquire greater potential energy during the fall, which leads to greater height in the rebound. The modeling assumes 3 meters in height and 2 meters in length from the base of the slope to the roadway.

The fall of mass portions of the slope generates a threat to the circulation of the avenue. Therefore, with the objective of mitigating the risk, a containment barrier can be provided by knowing the trajectory that describes the movement of the blocks. In Table 5, the geometry of two barriers in different positions is shown, from the most unfavorable situation raised from the slope, shown in the profile 3 of Fig. 6.

Table 5

Proposed containment solution. Modified on: Rocfall.

 <div data-bbox="422 499 561 607" style="border: 1px solid black; padding: 2px;"> <p>Barriers Start Point: 1, 0 End Point: 1, 3.2 Capacity: Infinite</p> </div>	<p>Option 1: A system of limitation of 1 meter from the base of the slope is proposed, with an elevation of 3.2 meters, retaining 100% of the blocks, which in their fall generate a maximum total energy of impact of 40 Jules (blocks falling directly to the barrier will have this energy). Also, due to the dissipation of energy in the rebound, it was observed that the greater amount of blocks represented only 10 Joules.</p> <p style="text-align: center;">Total Kinetic Energy on Barrier001</p>  <table border="1" data-bbox="628 622 1422 1043"> <caption>Data for Total Kinetic Energy on Barrier001</caption> <thead> <tr> <th>Location (m)</th> <th>Number of Rocks</th> </tr> </thead> <tbody> <tr><td>0</td><td>28</td></tr> <tr><td>2</td><td>9</td></tr> <tr><td>4</td><td>7</td></tr> <tr><td>6</td><td>2</td></tr> <tr><td>35</td><td>1</td></tr> <tr><td>38</td><td>2</td></tr> <tr><td>40</td><td>1</td></tr> </tbody> </table>	Location (m)	Number of Rocks	0	28	2	9	4	7	6	2	35	1	38	2	40	1																				
Location (m)	Number of Rocks																																				
0	28																																				
2	9																																				
4	7																																				
6	2																																				
35	1																																				
38	2																																				
40	1																																				
 <div data-bbox="355 1283 558 1368" style="border: 1px solid black; padding: 2px;"> <p>Barriers Start Point: -0.306213, 0.895264 End Point: 1, 3 Capacity: Infinite</p> </div>	<p>Option 2: The barrier is contemplated with an initial point of 30 cm towards the slope and 90 cm elevated from the base with an inclination towards the road so that this one does not exceed 1 meter horizontally, and 3 meters of height; retaining 100% of the sample. The total impact energy is approximately 38 Joules.</p> <p style="text-align: center;">Total Kinetic Energy on Barrier002</p>  <table border="1" data-bbox="628 1395 1422 1783"> <caption>Data for Total Kinetic Energy on Barrier002</caption> <thead> <tr> <th>Location (m)</th> <th>Number of Rocks</th> </tr> </thead> <tbody> <tr><td>35.0</td><td>2</td></tr> <tr><td>35.2</td><td>2</td></tr> <tr><td>35.4</td><td>2</td></tr> <tr><td>35.6</td><td>1</td></tr> <tr><td>35.8</td><td>3</td></tr> <tr><td>36.0</td><td>3</td></tr> <tr><td>36.2</td><td>5</td></tr> <tr><td>36.4</td><td>3</td></tr> <tr><td>36.4</td><td>6</td></tr> <tr><td>36.6</td><td>1</td></tr> <tr><td>36.6</td><td>4</td></tr> <tr><td>36.8</td><td>6</td></tr> <tr><td>37.0</td><td>4</td></tr> <tr><td>37.2</td><td>1</td></tr> <tr><td>37.4</td><td>3</td></tr> <tr><td>37.6</td><td>1</td></tr> <tr><td>37.8</td><td>2</td></tr> </tbody> </table>	Location (m)	Number of Rocks	35.0	2	35.2	2	35.4	2	35.6	1	35.8	3	36.0	3	36.2	5	36.4	3	36.4	6	36.6	1	36.6	4	36.8	6	37.0	4	37.2	1	37.4	3	37.6	1	37.8	2
Location (m)	Number of Rocks																																				
35.0	2																																				
35.2	2																																				
35.4	2																																				
35.6	1																																				
35.8	3																																				
36.0	3																																				
36.2	5																																				
36.4	3																																				
36.4	6																																				
36.6	1																																				
36.6	4																																				
36.8	6																																				
37.0	4																																				
37.2	1																																				
37.4	3																																				
37.6	1																																				
37.8	2																																				

There are advantages and disadvantages involved in the decision to opt for one or another proposed location. If option 1 were considered, its benefit would lie in the ease of cleaning, since the rocks would be deposited at the level of the base, and the construction of the barrier

with the technique of interest chosen by the designer, would be easier because of its perpendicularity to the ground. However, its design must be studied in detail, because if a total retention of the block is intended, the barrier would work mostly at 25% of its capacity.

On the other hand, if option 2 is considered, given the geometry observed in the graph on the left of Table 5, it is more difficult to build and maintain. Although, it can be considered for cases in which the circulation area is adjacent to the foot of the slope.

5. DISCUSSIONS AND CONCLUSIONS

To have road communication between the south and northeast of the city of Guayaquil, the San Eduardo tunnel was built in the sector known by the same name; For this construction of the access to the Modesto Apolo Ramírez Avenue was required, and implied cutting slopes due to the topography of the sector.

The steep slopes of the hill did not generate a threat at the time of the foundation, and as can be seen in the analysis proposed in this document (RMR, SMR and Q-Slope), there is a competent mass. However, in recent months there has been evidence of a large volume of blocks detaching from the solid mass and generate a risk for vehicles and passers-by that circulate on the avenue.

As a preventive measure, the local authorities have opted to divert vehicle traffic on a single lane, away from the area affected. Also, it was included the analysis of falling rocks and schematic solutions for retention barriers by Rocfall Software, which proposes an interesting modeling to predict the impact in distance and design a solution that enables the use of the road in its entirety.

This study analyzed the problems and causes of instability, but not the design of corrective measures. Even though, it was presented some geometric solutions. To design the complete reinforcement of the slope and analyze the different construction alternatives, it was necessary to perform the kinematic analysis of failure by wedge, overturning and planar breakage with the angle of friction of the site. Additionally, the study proposes the dimensions and geometric disposition of the barrier. Nevertheless, the appropriate technology should be sought, and aligned with a budget that makes implementation possible by optimizing resources thus, making it possible to transit without the current risk posed by the slope.

ACKNOWLEDGEMENTS

This research has been developed as a work of completion of the Master in Geotechnics of the Faculty of Engineering and Earth Sciences of the Escuela Superior Politécnica del Litoral - ESPOL, approved by the CES under resolution RPC-SO-20-No.292 -2018 Program: 750732C01. Special thanks to Daniel Garcés for his support in the cartographic information. Thanks to Davide Besenon for his suggestions on the topics of research and guidance.

Alexandra Macías

Dálida Vera

CONFLICT OF INTEREST

Luis Jordá, Alexandra Macías, Kaymara Vera and César Patricio Borja declare that he has no conflict of interest.

FINANCING

This research did not receive any specific grants from funding agencies in the public, commercial, or non-profit sectors.

REFERENCES

- Anbalagan R, Sharma S, Raghuvanshi TK. Rock mass stability evaluation using modified SMR approach. In: Jha, P.C. (Ed.), *Rock Mechanics Proceedings of the Sixth National Symposium on Rock Mechanics 1992*;258–68.
- Aksoy H, Ercanoglu M. Determination of the rockfall source in an urban settlement area by using a rule-based fuzzy evaluation. *Natural Hazards and Earth System Science* 2006;6(6):941–54. <https://doi.org/10.5194/nhess-6-941-2006>
- Bar N, Barton N. Empirical slope design for hard and soft rocks using Q-slope. In: *Proceedings of the 50th US rock mechanics/geomechanics symposium, ARMA 2016, Houston, 26–29 June 2016* 2016;ARMA(16):384
- Bar N, Barton N. The Q-Slope Method for Rock Slope Engineering. *Rock Mech Rock Eng* 50 2017:3307–22. <https://doi.org/10.1007/s00603-017-1305-0>
- Barton N, Lien R, Lunde J. Engineering classification of rock masses for the design of tunnel support. *Rock Mechanics* 1974;6:189–236. <https://doi.org/10.1007/BF01239496>
- Basahel H, Mitri H. Application of rock mass classification systems to rock slope stability assessment: A case study. *Journal of Rock Mechanics and Geotechnical Engineering* 2017;9(6): 993–1009. <https://doi.org/10.1016/j.jrmge.2017.07.007>
- Bieniawski ZT. Engineering classification of jointed rock masses. *En Trans. South Afr. Inst. of Civ. Eng* 1973;15:355-344.
- Bieniawski ZT. Rock mass classification in rock engineering. *En Proc. Symp. on Exploration for Rock Eng. Balkema, Rotterdam* 1976;1:97-106.
- Bieniawski ZT. The Geomechanics Classification in rock engineering applications. *En Proc. 4th Int. Cong. On Rock Mech. ISRM Montreux. Balkema.* 1979;5:55-95.
- Bieniawski ZT. *Engineering Rock Mass* Wiley, New York 1989.
- Bristow CR, Roger C. The age of the Cayo Formation, Ecuador. *Newsletters on Stratigraphy* 1976;4(3):169–73. <https://doi.org/10.1127/nos/4/1976/169>
- Bristow CR, Hoffstetter R. *Lexique stratigraphique international: Amérique Latine. Ecuador:(incl. Galapagos). Centre National de la Recherche Scientifique* 1977.
- Deere DU, Deere DW. The rock quality designation (RQD) index in practice. In *Rock classification systems for engineering purposes*, (ed. L. Kirkaldie), ASTM Special Publication. Philadelphia: Am. Soc. Test. Mat.1988;984:91-101.
- Deere DU. Rock quality designation (RQD) after 20 years. U.S. Army Corps Engrs Contract Report GL-89-1. Vicksburg, MS: Waterways Experimental Station 1989.
- Fernández-Gutiérrez JD, Pérez-Acebo H, Mulone-Andere D. Correlación entre el índice RMR de Bieniawski y el índice Q de Barton en formaciones sedimentarias de grano fino. *Informes de La Construcción* 2017;69(547). <https://doi.org/10.3989/id54459>

- Guzzetti F, Reichenbach P, Wieczorek GF. Rockfall hazard and risk assessment in the Yosemite Valley, California, USA. *Natural Hazards and Earth System Science* 2003;3(6):491–503. <https://doi.org/10.5194/nhess-3-491-2003>
- Hantz D, Vengeon JM, Dussauge-Peisser C. Natural Hazards and Earth System Sciences An historical, geomechanical and probabilistic approach to rock-fall hazard assessment. *Natural Hazards and Earth System Sciences* 2003;3:693–701.
- Hoek E. Analysis of rockfall hazards Introduction. In *Practical Rock Engineering* 2000:1–25.
- Hoek, E., & Bray, J. D. (1981) *Rock slope engineering*. CRC Press, 3rd edition. Institution of Mining and Metallurgy. Taylor and Francis, 23
- Instituto Geográfico Militar. Catálogo de Datos del IGM Ecuador - Instituto Geográfico Militar del Ecuador. [Geoportaligm.gob.ec](http://www.geoportaligm.gob.ec). Retrieved 1 October 2020. <http://www.geoportaligm.gob.ec/geonetwork/srv/spa/catalog.search;jsessionid=212DBD7A9FA6F8070B68B9D376937FA2#/metadata/5c478da0-cc83-4aff-ab6a-d7129e8a6e33>.
- Jordá-Bordehore L. Application of Q slope to Assess the Stability of Rock Slopes in Madrid Province, Spain. *Rock Mechanics and Rock Engineering* 2017;50(7):1947–57. <https://doi.org/10.1007/s00603-017-1211-5>
- Jordá-Bordehore L, Jordá-Bordehore R, Durán Valseo JJ, Romero-Crespo PL. Evaluación de la estabilidad de las labores y pilar corona en las minas abandonadas de S'Argentera (Ibiza, España) combinando clasificaciones geomecánicas, métodos empíricos y análisis numérico-enfocado a su posible aprovechamiento turístico. *Boletín Geológico y Minero* 2017; 128(1):3–24. <https://doi.org/10.21701/bolgeomin.128.1.001>
- Labrousse B. (1986). Relaciones entre la Formación Cayo y la Formación Piñón en el sector de Guayaquil. Implicaciones Geodinámicas. *Cultura: Revista del Banco Central del Ecuador*, Coloquio Ecuador 86, Quito 1986:12.
- Lahmeyer International. Resumen ejecutivo Diseño de los túneles San Eduardo 2006.
- Navarrete E. Itinerarios Geológicos de la costa del Ecuador 1 Guayaquil y sus alrededores, Guayaquil 2018:2-31
- Palmstrom A, Broch E. Use and misuse of rock mass classification systems with particular reference to the Q-system. *Tunnelling and Underground Space Technology* 2006;21(6):575–93. <https://doi.org/10.1016/j.tust.2005.10.005>
- Pantelidis L. Rock slope stability assessment through rock mass classification systems. *International Journal of Rock Mechanics and Mining Sciences* 2009;46(2):315–25. <https://doi.org/10.1016/j.ijrmms.2008.06.003>
- Rocscience. *RockFall User's Guide* 2002.
- Romana M. New adjustment ratings for application of Bieniawski classification to slopes. *Proc. Int. Symp. on the Role of Rock Mechanics* 1985:49-53.
- Romana M. The geomechanical classification SMR for slope correction. *Proc. Int. Congress on Rock Mechanics* 1995;3:1085-92.

- Romana, Manuel & Serón, José & Montalar, Enrique. La clasificación geomecánica SMR: aplicación experiencias y validación. V Simposio Nacional sobre Taludes y Laderas Inestables – Madrid 2001:393-404.
- Romana M, Serón JB, Montalar E. SMR geomechanics classification: application, experience and validation. In: Merwe, J.N. (Ed.), Proceedings of the 10th Congress of the International Society for Rock Mechanics, ISRM 2003—Technology Roadmap for Rock Mechanics. South African Institute of Mining and Metallurgy 2003:1–4.
- Umrao RK, Singh R, Ahmad M, Singh TN. Stability Analysis of Cut Slopes Using Continuous Slope Mass Rating and Kinematic Analysis in Rudraprayag District, Uttarakhand. Geomaterials 2011;01(03):79–87. <https://doi.org/10.4236/gm.2011.13012>.

FIGURES INDEX

Figure 1. Orthophoto of the study area.	¡Error! Marcador no definido.
Figure 2. Location map of the study area with the characteristic geological formation. Modified on: Instituto Geográfico Militar, 2020. 3	
Figure 3. Drop path of 50 blocks of 0.3 Kg. Modified on: Rocfall program.	7
Figure 4. Diagram of pole density and breakage typologies with representative photographs of the stations. Modified on: Dips 6.0 program.	9
Figure 5. Presentation of the stability of the slopes of each geomechanical station. Modified on: Barton and Bar, 2017.....	¡Error! Marcador no definido.
Figure 6. Schematic and block range distribution of the Geomechanical Stations. Modified on: Rocfall.	¡Error! Marcador no definido.

TABLE INDEX

Table 1. Seal adjustment factors by SMR method. Modified from Romana (1985) by Anbalgan et al (1992).....	5
Table 2: Stability classes and classification of rocky slopes according to SMR (Romana, 1985).	5
Table 3. RMR Classification Results.....	¡Error! Marcador no definido.
Table 4. Results of SMR and Q-slope systems for the Cerro San Eduardo - Guayaquil slope stations.....	¡Error! Marcador no definido.
Table 5. Proposed containment solution. Modified on: Rocfall. .	¡Error! Marcador no definido.